

# Reducing Uncertainties Regarding Remaining Lives of Structures Using Computer-aided Data Interpretation

ROMAIN PASQUIER, JAMES-A. GOULET, IAN F. C. SMITH  
Applied Computing and Mechanics Laboratory (IMAC)  
School of Architecture, Civil and Environmental Engineering (ENAC)  
ÉCOLE POLYTECHNIQUE FÉDÉRALE DE LAUSANNE (EPFL)  
Lausanne, Switzerland  
rpasquie@gmail.com

The growing importance of economic and environmental issues associated with the replacement of transportation infrastructure creates a demand for new techniques that are able to predict accurately the behaviour of existing structures. While monitoring structural behaviour can help reduce uncertainties, measured data alone is not sufficient to determine the behaviour of a structure. Models are necessary to infer causes from measurements and to perform prognostics because direct measurements are often not able to indicate causes directly. Furthermore, due to the large amount of data involved, it is in most cases not possible to process it without relying on automated computer-aided interpretation approaches. This paper presents a methodology that can improve the prognosis of complex systems by reducing uncertainties stress range predictions. An example made on a full-scale bridge shows the applicability and the benefits of the methodology for the prognosis of stresses used in the determination of the remaining fatigue life.

## 1. Introduction

In recent years, measuring instrument technologies evolved quickly so that it is now possible to use a large number of cheap and reliable devices. However, it is still not possible to measure every component of complex structures in every direction. The extrapolation of the response at the unmeasured components is made via behavioural models. Experience shows that for current structures, there are often important differences between predictions from *design models* and measured behaviour. These differences are often due to epistemic uncertainties associated with the idealization of the reality. System-identification methodologies help find models that are able to predict the real behaviour of structures.

During the evaluation of existing structures, and in the absence of detected damage, limit-state verifications are first performed using conservative design-stage models. If design-stage models are adequate and the performance is acceptable, no site intervention is required. In cases where the performance is inadequate, conservative design practices can be improved upon using information obtained from site investigations. For example, measurements can be used to improve behaviour models using system identification. If refined models lead to a conclusion of sufficient performance, no further intervention is required. Otherwise, engineers might perform additional site investigations, refine limit-state requirements using more sophisticated reliability analyses or they may proceed with interventions on structures. Interventions involve actions such as structural improvements, replacement of elements and complete structural replacement. Often, large structures are replaced unnecessarily, at tremendous cost, due to traditional practices. Occasionally, the reverse situation occurs; design models that are no longer relevant lead to bad structural assessments involving non-conservative performance levels and this increases the risk of structural collapse. Here, the cost to society could be much greater than the cost of unnecessary structural replacement.

System identification involves determining unknown characteristics of behavioural models from observations. The most common data-interpretation technique is residual minimization, also known as curve fitting, model-calibration and model-updating. This type of approach calibrates the parameters of a model in order to minimize the discrepancy between predicted and measured values. However, according to ASME guideline for verification and validation (2006), calibrated models are valid only for measurements used. It is usually inadequate for predicting the behaviour outside the domain of the data collected, and even less for use in other analyses. Another approach is the Bayesian updating (Beck and Katafygiotis, 1998). This technique updates the prior knowledge on model parameters using measurements according to Bayesian conditional probability. The likelihood function used is commonly based on a residual minimization criterion.

One purpose for identifying systems is to make prognoses with respect to future performance, including the evolution in model inputs, such as loading as well as structural deterioration, future hazard scenarios, change of function and new environmental variables due to climate change (for example, wind and snow loading). Several approaches currently exist for assessing the remaining life and reliability of systems. For instance, Okasha et al. (2012) calibrated model parameters of a bridge using residual minimization to improve degradation models used in the calculation of the remaining capacity assessment of structures. Many authors rated structures and performed prognostics on future performance using models that were validated without using data-interpretation techniques (Wang et al. (2011a, 2011b), Siriwardane et al. (2008)).

Current fatigue prognostic techniques use the weigh-in-motion load quantification techniques and strain measurements taken at critical regions to identify stress amplitudes and the loading history. However, it is not feasible to measure everywhere. Also, it is difficult to forecast the evolution of the remaining fatigue life under either increased traffic or when modifications are made on the structure. For these situations, engineers need to rely on behaviour models. During remaining fatigue life assessment, the accuracy of stress-range predictions is crucial for quantifying fatigue damage.

Model-based data interpretation approaches allow uncertainties associated with the evaluation of stress predictions to be included. In welded structural connections, reducing stress amplitudes by 50% can lead to an eight-fold gain in fatigue life. A better knowledge of uncertainties related to these amplitude predictions could lead to a better quantification of the fatigue limit state. Few studies have been conducted with computer-aided measurement-data interpretation methodologies, where uncertainties are explicitly included in fatigue evaluations. New alternatives are made possible by recent advances in computing power that enable processing of populations of candidate solutions.

This paper proposes a new approach to perform prognosis on civil structures. Section 2 reviews the model falsification methodology used to improve the understanding of behaviour models using measurements taken on the structure. Section 3 describes the methodology used to perform prognostics using field-data. Section 4 presents a case study where the applicability and benefits of the approach are illustrated.

## **2. Error-domain model falsification**

Goulet and Smith (2011, 2012) proposed a solution for shortcomings of current methodologies and more specifically for cases where uncertainties cannot be exactly defined.

The approach proposed is named error-domain model falsification. In order to represent the behavior of the real system, a model  $\mathbf{g}(\dots)$  is created among several possible classes of model. This model takes as input a set of  $n_p$  physical parameters  $\boldsymbol{\theta} = [\theta_1, \theta_2, \dots, \theta_{n_p}]^T$  describing the geometrical and material unknown characteristics of the system. Error-domain model falsification is based on the comparison of predicted and measured values. Equation 1 presents the general formulation used to compare predicted and measured quantities.

$$\mathbf{g}_i(\boldsymbol{\theta}) - \epsilon_{model,i}^* = y_i - \epsilon_{measure,i}^* \quad (1)$$

The observed residual represents the discrepancy between the predicted value  $\mathbf{g}_i(\boldsymbol{\theta})$  an observed value  $y_i$ , where  $i$  corresponds to the location where these values are compared ( $i \in \{1, \dots, n_m\}$ ). Errors, originating from both the model ( $\epsilon_{model,i}^*$ ) and measurements ( $\epsilon_{measure,i}^*$ ), are represented by random the variables  $U_{model,i}$  and  $U_{measure,i}$ . The model uncertainties are, for example, due to the geometric variability of the structure, the variability of material properties and mesh-refinement uncertainty of the finite-element model. These uncertainties are estimated through the evaluation of model-prediction variance. Model-simplification uncertainties are estimated using engineering heuristics. Measurement uncertainties are due to sensor resolution, cable losses and measurement repeatability. These sources of uncertainties are estimated based either on manufacturer specifications or domain heuristics. All of these uncertainties are combined to obtain a random variable  $U_{c,i}$  representing possible outcomes of the differences between predicted and measured values.

A model instance is falsified if, for any measurement location, the difference between predicted and measured values is outside the interval defined by threshold bounds  $[T_{low,i}, T_{high,i}]$  (see Equation 2). A model instance is thus accepted only if this difference lies inside the bounds at every location  $i$ .

$$\forall i \in [1, \dots, n_m]: T_{low,i} \leq \mathbf{g}_i(\boldsymbol{\theta}) - y_i \leq T_{high,i} \quad (2)$$

Threshold bounds are determined specifically for every location  $i$  based on the combined uncertainty probability distribution function  $f_{U_{c,i}}(\epsilon_{c,i})$ . They define the shortest intervals including simultaneously a target probability  $\varphi$  and satisfying Equation 3. The value  $\varphi$ , is the probability that the right model remains in the candidate model set after falsification. This way of defining threshold bounds also uses the Sidak correction, which accounts for the effects of the comparison of models with multiple measurements (Sidak, 1971). It has the advantage of providing conservative threshold bounds, regardless of the dependencies between uncertainties (JCGM, 2011).

$$\forall i \in \{1, \dots, n_m\}: \varphi^{\frac{1}{n_m}} = \int_{T_{low,i}}^{T_{high,i}} f_{U_{c,i}}(\epsilon_{c,i}) d\epsilon_{c,i} \quad (3)$$

All models that remain non-falsified are kept in the candidate model set. This set contains models that are possible explanations of all measurements while accounting for modelling and measurement uncertainties. Prognostics are then based on the predictions of the candidate model set.

### 3. Methodology

With recent advances in computing power, it is now possible to identify and perform prognostics for populations of solutions. Instead of basing prognostics on a single model class

and on a single set of parameter values, all candidate models identified (see Section 2) are used to provide lower and upper bounds for predicted values.

For fatigue prognosis, a number of cycles under constant stress-range level are employed to evaluate the cumulative damage index. Histograms of cyclic stresses are obtained from either measured or simulated traffic. The fatigue damage spectrum is obtained using a Rainflow analysis (Fisher et al., 1998). Miner's rule (Miner, 1945) established that the damage  $D$  produced by the stress ranges  $\Delta S_i$  and the number of cycles  $n_i(\Delta S_i)$  can be added for each stress magnitude number  $i \in \{1, \dots, k\}$  in the spectrum. This damage index is expressed in Equation 4 where  $N_i$  is the number of cycles to failure considering appropriate fatigue S-N curves. Fatigue failure is expected when the damage index reaches a value of 1.

$$D = \sum_{i=1}^k \frac{n_i(\Delta S_i)}{N_i} \leq 1 \quad (4)$$

Predicted stress-cycle amplitudes are determined by using simulated traffic loading within the behaviour models. Traffic loads are decomposed in truck-axle loads. The stress predictions  $S_i$  for a single axle load are extracted from the candidate finite-element models and influence lines are established for critical truss connections (see Figure 1). Influence lines are computed by applying axle loading at discrete locations. Then, stresses for any load position are interpolated using regression analysis. Because these influence lines have to be determined for every candidate model, this interpolation technique allows computing resources to be used more efficiently. The influence lines are interpolated using polynomial functions (see Equation 5), where the order of the polynomial is  $m$ . The residual  $\epsilon_{sa}$  of the interpolation is estimated in order to be included in the definition of thresholds.

$$S(x) = a_0 + a_1x + a_2x^2 + a_3x^3 + \dots + a_mx^m + \epsilon_{sa} \quad (5)$$

An influence line gives the stress prediction at one point for any position of the axle load on the structure. With the principle of linear superposition, these stress predictions are extrapolated for simulated traffic loading, so that a stress history for each critical connection is available. A Rainflow analysis (Fisher et al., 1998) is performed to determine the number of cycles associated with each stress range. These stress ranges are used as inputs in the cumulative damage index to evaluate the remaining fatigue life of each critical connection.

By reducing uncertainties related to the prediction of stress cycles, the reserve capacity of the structure can be quantified more accurately. In Section 4, an application of this methodology is presented. The process is limited to the calculation of stress predictions for a single position of axle load.

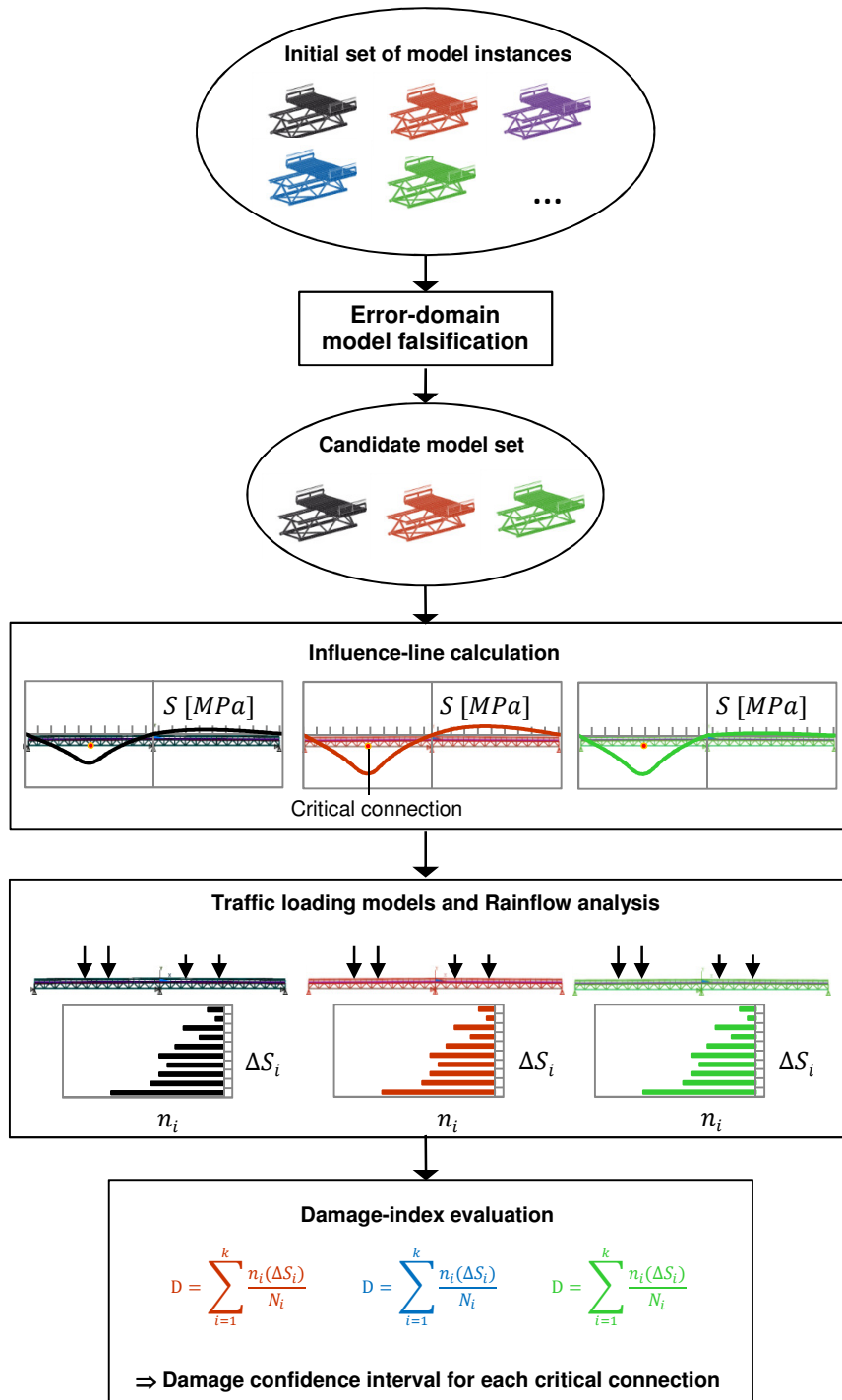


Figure 1– Methodology flowchart

#### 4. Application

In this example, a composite steel-concrete bridge, located in Aarwangen (Switzerland) is studied. The bridge is made of welded steel trusses acting in a composite manner with the concrete deck. Figure 2 shows the cross-section of the finite-element model of the structure. The ultimate goal of this study is to evaluate the reserve fatigue capacity of tubular welded connections.

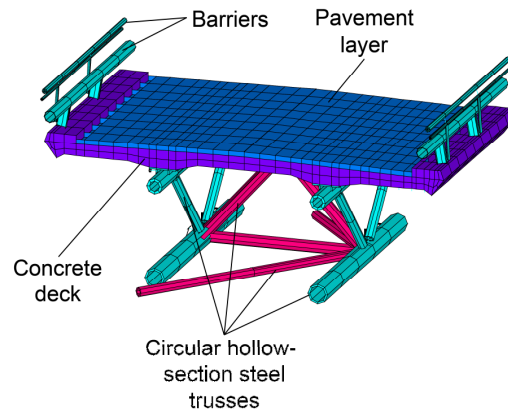


Figure 2 – Aarwangen Bridge model cross-section

Several characteristics of the structure are unknown, such as, the rotational stiffness of the truss connections and the longitudinal stiffness of the pavement covering expansion joints. The rotational stiffness of the truss connections is represented by rotational springs connected between the diagonal members and either the upper or lower chord. Expansion joints are modelled using springs parallel to the bridge longitudinal axis. Possible parameter values for spring stiffness are sought for both the southern and northern abutments.

The data of three static-load tests are used to identify the value of unknown parameters. The initial model set is generated using values of three primary parameters: the stiffness of the truss connections and the stiffness of two expansion joints. Previous analyses have shown that elastic moduli have a lesser influence on the structure behaviour than these parameters. The ranges of values for the spring stiffness were determined by a sensitivity analysis. Primary-parameters  $\theta$  and their possible values are presented in Table 1. Parameter samples are used to build an initial model set containing 1000 instances.

Table 1 – Initial model set parameter ranges and discretization intervals

Primary parameter $\theta$	Units	Range	Number of discretization intervals
Rotational stiffness of truss connections	MNm/rad	0.1-1000	10
Stiffness of southern expansion joint	MN/m	0-1000	10
Stiffness of northern expansion joint	MN/m	0-1000	10

Values for  $U_{model,i}$  and  $U_{measure,i}$  are estimated based on uncertainty sources, see Tables 2 and 3. These values are determined using field data and by engineering experience.

Table 2 – Secondary parameter variability

<b>Model uncertainty source</b>	<b>Units</b>	<b>PDF</b>	<b>Mean/Min</b>	<b>STD/Max</b>
$\Delta\nu$ Poisson's ratio of concrete	-	Gaussian	0.19	0.025
$\Delta t_1$ main steel plates	%	Gaussian	0	1
$\Delta t_2$ steel plates	%	Gaussian	0	1
$\Delta t$ pavement thickness	%	Gaussian	0	5
$\Delta W$ truck axle weight	kN	Uniform	-5	5
Elastic modulus of pavement	MPa	Gaussian	10000	3000
Elastic modulus of steel	MPa	Gaussian	210000	6000
Elastic modulus of concrete	MPa	Gaussian	35000	4000

Table 3 – Other uncertainty sources

<b>Uncertainty source</b>	<b>Units</b>	<b>PDF</b>	<b>Mean/Min</b>	<b>STD/Max</b>
Sensor resolution	$\mu\text{mm/mm}$	Uniform	-2	2
Cable losses	%	Uniform	-1.3	1.3
Model simplifications and FEM	%	Uniform	-10	20
Mesh refinement	%	Uniform	-2	0
Additional uncertainty	%	Uniform	-1	1
Repeatability	%	Gaussian	0	1.5
Truck position	%	Uniform	-3	3

Given that the primary parameter values are varied explicitly during sampling, Figure 3 presents the relative importance of the remaining uncertainties on the threshold-bound calculation. The uncertainty on secondary parameters contributes the most to this uncertainty.

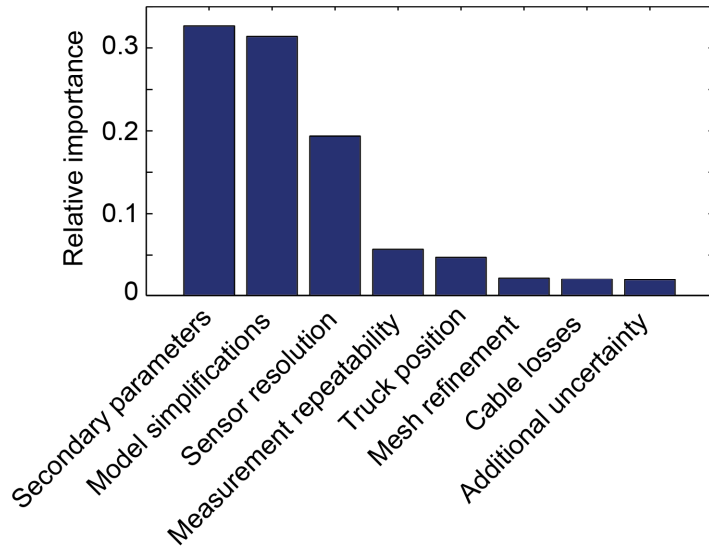


Figure 3 – Relative importance of uncertainty sources

For a target probability  $\varphi = 0.95$ , error-domain model falsification reveals 27 candidate models based on the comparison of six strain measurements. Figure 4 presents the initial-model-set predictions for a strain measurement location. The continuous line represents the measured value and the dashed lines, the threshold bounds that are defined based on the combined uncertainty probability density function. Each dot corresponds to the prediction of a model instance and the candidate models are represented by crosses. Falsified models included in threshold bounds are rejected by comparisons at other measurement locations.

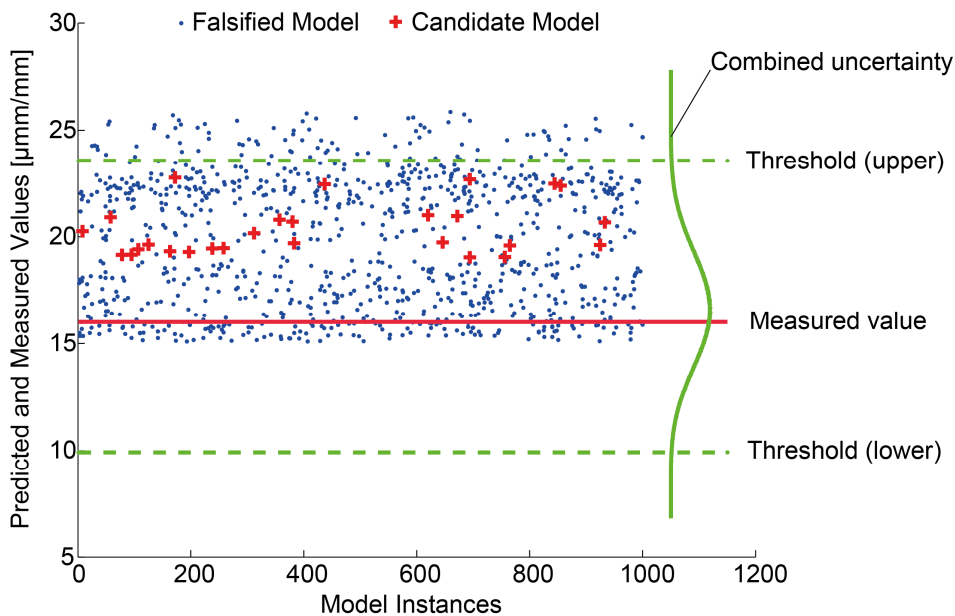


Figure 4 – Candidate-model plot for a strain measurement location

The results show that the model takes any parameter value for the north expansion joint stiffness. For the south expansion joint stiffness, the accepted values are between 0 and 5.6 MN/m compared with an initial possible range of 0 to 1000 MN/m. Although the 0-value is possible for both joints, a stiffening effect of the expansion joint cannot be excluded. Additional measurements are needed to quantify more precisely the properties of these boundary conditions. All candidate models have values for the rotational stiffness of the truss connection in the middle of the possible range. Specifically these are to values between 2.15



MNm/rad and 359 MNm/rad, compared with an initial possible range of 0.1 to 1000 MNm/rad. This indicates that strain predictions are more sensitive to truss connection stiffness. Moreover, perfectly rigid truss connections, as it is often assumed in design models, are not representative of the real structure behaviour. For prognosis purposes, such models could yield biased stress ranges.

The 27 candidate models are used to predict stresses as described in the methodology presented in Section 3. This paper is limited to the scope of predicting stresses for a single location on the structure. Stresses are calculated by applying a truck axle of 100 kN centred on the west lane of the bridge. Figure 5 presents the connection locations for which the stresses are evaluated. In order to illustrate the potential of the prognosis methodology, stress predictions obtained using the candidate model set are compared with those obtained by the entire initial model set and with the predictions of a single model using design values. The results are presented in Figure 6.

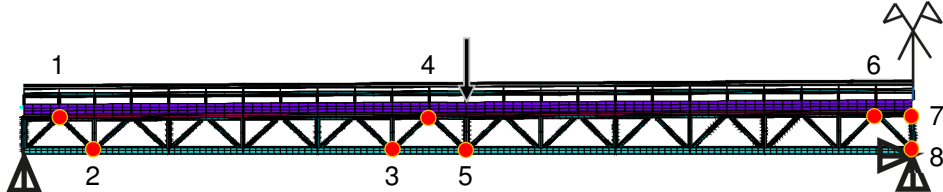


Figure 5 – Critical truss connection locations

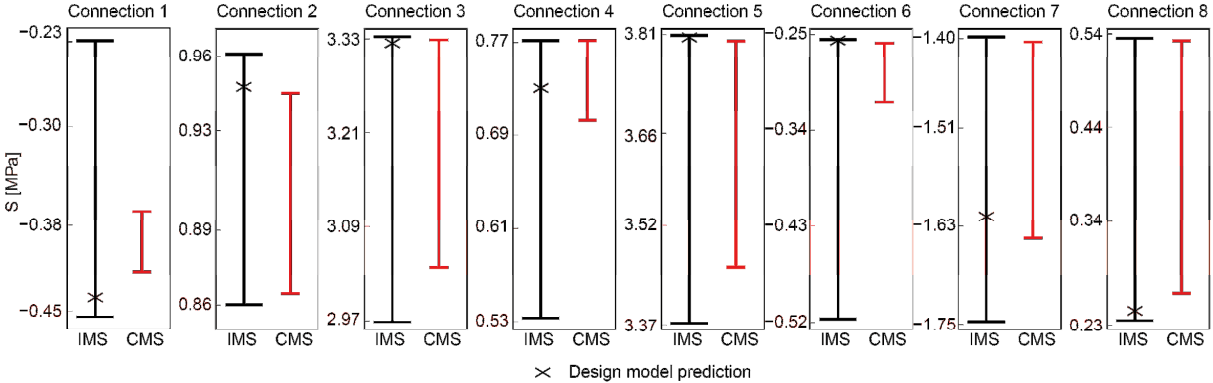


Figure 6 – Comparison of stress predictions between the initial model (IMS) set and the candidate model set (CMS), as well as model predictions made using design values for each critical truss connections

The stress interval reduction is up to 78% for the truss connections number 1 and 6, as well as 71% for connection 4. For the other connections, the reduction varies between 10% and 31%. These percentages represent a reduction of the prediction intervals of the candidate model set compared with the initial model set. Moreover, the predictions made using design values, for connection 1, 2 and 8, are outside of the candidate-model-set interval. For connections 8, the model using design values returns non-conservative stress predictions, while over-conservative stress predictions are obtained for connections 1 and 2. Measurements thus improve model-prediction accuracy.

## 5. Conclusion

In this paper, a methodology is presented to improve prognosis using model-based data-interpretation. Error-domain model falsification is used to identify the values of model parameters. The candidate models obtained are then used to predict stress ranges under a traffic load model. For the bridge tested, a reduction in predicted stress is observed after falsification of inadequate models using static measurements. In this case, stresses under a single axle load were reduced up to 78%. Also, it is shown that predictions made using design values can be over-conservative and in some case non-conservative compared with predictions obtained using model-based data interpretation. In the context of road network management, the amount of information to be interpreted is too large to be processed manually. This computer-aided data-interpretation methodology offers the possibility to use populations of models to perform better prognostics.

## References

- ASME 2006. Guide for Verification and Validation in Computational Solid Mechanics. *ASME, New York*, 28p.
- BECK, J. L. & KATAFYGIOTIS, L. 1998. Updating models and their uncertainties. I: Bayesian statistical framework. *Journal of Engineering Mechanics*, 124, 455-461.
- FISHER, J. W., KULAK, G. L. & SMITH, I. F. C. 1998. A Fatigue Primer for Structural Engineers. *National Steel Bridge Alliance*, 130p.
- GOULET, J.-A. & SMITH, I. F. C. 2011. Prevention of over-instrumentation during the design of a monitoring system for static load tests. In *5th International Conference on Structural Health Monitoring on Intelligent Infrastructure (SHMII-5)*. Cancun, Mexico.
- GOULET, J.-A. & SMITH, I. F. C. 2012. Predicting the Usefulness of Monitoring for Identifying the Behavior of Structures. *Journal of Structural Engineering*, in press.
- JCGM 2011. Evaluation of measurement data - Supplement 2 to the "Guide to the expression of uncertainty in measurement" - Extension to any number of output quantities. *JCGM Working Group of the Expression of Uncertainty in Measurement*, JCGM 102, 72p.
- MINER, M. 1945. Cumulative fatigue damage. *ASME Journal of Applied Materials*, 12, A159-A164.
- OKASHA, N. M., FRANGOPOL, D. M. & ORCESI, A. D. 2012. Automated finite element updating using strain data for the lifetime reliability assessment of bridges. *Reliab. Eng. and Syst. Saf.*, 99, 139-150.
- SIDAK, Z. 1971. On probabilities of rectangles in multivariate Student distributions: their dependence on correlations. *The Annals of Mathematical Statistics*, 169-175.
- SIRIWARDANE, S., OHGA, M., DISSANAYAKE, R. & TANIWAKI, K. 2008. Application of new damage indicator-based sequential law for remaining fatigue life estimation of railway bridges. *Journal of Constr. Steel Res.*, 64, 228-237.
- WANG, N., ELLINGWOOD, B. R. & ZUREICK, A.-H. 2011a. Bridge Rating Using System Reliability Assessment. II: Improvements to Bridge Rating Practices. *Journal of Bridge Engineering*, 16, 863-871.
- WANG, N., O'MALLEY, C., ELLINGWOOD, B. R. & ZUREICK, A.-H. 2011b. Bridge Rating Using System Reliability Assessment. I: Assessment and Verification by Load Testing. *Journal of Bridge Engineering*, 16, 854-862.